MATHEMATICAL MODELING AND STATIC ANALYSIS OF GUYED STEEL TOWERS SUBJECTED TO WIND ACTION

https://doi.org/10.63330/aurumpub.043-008

Evandro de Carvalho Ribeiro[1], Francisco Arlon de Oliveira Chaves[2], Francisca das Chagas Oliveira[3], Andreson de França Almeida[4] and Eugenia Maria dos Santos Cordeiro[5]

Abstract

This study presents a numerical investigation of guyed steel tower structures with square cross-sections, used in telecommunication systems and subjected to static wind action. The procedures adopted to determine the static wind forces follow the methodology established in the Brazilian Standard NBR 6123. For the numerical study, the guyed towers were modeled using linear and nonlinear mathematical formulations that allow the introduction of prestressing forces in the cable elements, as well as the effects of temperature variation. These models were implemented in four computational programs developed by Menin, and the results obtained were compared with those from the commercial program SAP2000.

Keywords: Guyed Towers, Monte Carlo Method, Dynamic Analysis, Nonlinear Analysis.

INTRODUCTION

Telecommunication towers are structures characterized by low self-weight, high slenderness and flexibility, and a system in which axial forces are predominant. These characteristics, combined with the rare occurrence of earthquakes in Brazil, make them susceptible to wind action, which becomes the determining factor for design.

[1] Master, UnB, Brazil
E-mail: eng.prof.evandro@gmail.com
[2] Master, IFPI, Brazil
E-mail: arlonoliv@hotmail.com
[3] PhD Candidate, UFCG, Brazil
E-mail: engenheira.franoliv@gmail.com
[4] IFPI, Brazil
E-mail: andresonalmeida@ifpi.edu.br
[5] Specialist, UESPI, Brazil
E-mail: emscordeiro81@gmail.com

The guyed towers used in this analysis are lattice structures with square cross-sections. The main structure uses rolled equal-leg angle profiles properly joined by bolts. The cables used are of the EHS (Extra High Strength) type, composed of seven steel wires, and are discretized in the guyed towers only as a single element along their length.

For the performance of the static analysis, the prescriptions of the Brazilian standard NBR6123 were taken into account, subjecting the guyed towers to the wind loading proposed by the aforementioned standard (with perpendicular incidence relative to the tower face), as well as the self-weight and cable tensioning loads.

In the discretization of the structures, straight two-node finite elements (cables and trusses) are employed, assuming stiffness only in the axial direction. The material has linear elastic behavior, and the external forces act only at the nodes of the elements. The formulation allows elongations in the cable elements for the introduction of prestressing forces, according to two mathematical models:

- Nonlinear model for tensioned cable (Pulino);
- Linear model for tensioned cable (Pulino).

These models basically describe the derivation of the Total Potential Energy function of the system, so that the static equilibrium position is obtained by minimizing this function through a Quasi-Newton type algorithm.

To obtain the results of the static analysis of guyed steel towers of 10 m and 30 m in height, two computational programs developed by Menin are used. The programs employ the two mathematical formulations for linear and nonlinear analysis models used for two-node finite elements (cables and trusses).

NONLINEAR MODEL FOR TENSIONED CABLE

LONGITUDINAL STRAIN

In Figure 1, the undeformed configuration of a cable element is represented by segment AB, the tensioning by segment BC, and the thermal effect by BD, so that the undeformed cable, after undergoing the thermal effect, is represented by segment AD. The deformed configuration of the element, after undergoing the effect of the external nodal loads, is represented by segment A'C'. The nodal displacements AA' and CC' are indicated by the vectors p and q, respectively.

Figure 1

Nonlinear cable element model and vector representation

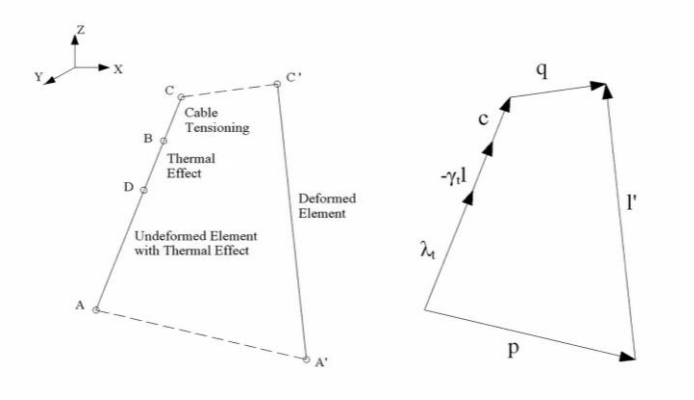

where:

$\lambda_c\lambda_c$: vector representing the distance between the nodes (segment AC);

l : vector representing the initial length of the cable (segment AB);

$\gamma_t l = \alpha \Delta T l \gamma_t l = \alpha \Delta T l$: thermal effect; ΔT the temperature variation;

$\lambda_t\lambda_t$: vector representing the undeformed configuration with thermal effect;

l' : vector with the deformed configuration;

p, q : nodal displacements at the initial and final ends;

$\mu = \|c\|\mu = \|c\|$: modulus of vector c;

$\boldsymbol{\mu_t} = \|\boldsymbol{\gamma_t l}\|\boldsymbol{\mu_t} = \|\boldsymbol{\gamma_t l}\|$: modulus of vector $\gamma_t l \gamma_t l$.

It can be verified from Figure 1 that:

$$p + l' = \lambda_t - \gamma_t l + c + qp + l' = \lambda_t - \gamma_t l + c + q \quad (1)$$

$$l' = \lambda_t - \gamma_t l + c + q - pl' = \lambda_t - \gamma_t l + c + q - p \quad (2)$$

Let:

$$z = q - p + c - \gamma_t lz = q - p + c - \gamma_t l \quad (3)$$

Thus:

$$l' = \lambda_t + zl' = \lambda_t + z \quad (4)$$

The longitudinal strain of the element can then be given by:

$$\varepsilon = \frac{\|l'\| - \|\lambda_t\|}{\|\lambda_t\|}\varepsilon = \frac{\|l'\| - \|\lambda_t\|}{\|\lambda_t\|} \quad (5)$$

Recalling that:

$$\|l'\| = \sqrt{(\lambda_t + z)^T(\lambda_t + z)}\|l'\| = \sqrt{(\lambda_t + z)^T(\lambda_t + z)} \quad (6)$$

being $\lambda_t = (\lambda_c - c + \gamma_t l) = L_t u \lambda_t = (\lambda_c - c + \gamma_t l) = L_t u \Rightarrow\Rightarrow$

$$\|\lambda_t\| = \|L_t u\| = L_t\|u\| = L_t\|\lambda_t\| = \|L_t u\| = L_t\|u\| = L_t \quad (7)$$

where u is the vector of the direction cosines of the cable element in the undeformed configuration and L_t o the undeformed length of the cable with thermal effect.

Therefore, substituting (7) into (6):

$$\|l'\| = \sqrt{{L_t}^2 u^T u + L_t u^T z + z^T L_t u + z^T z} \|l'\| = \sqrt{{L_t}^2 u^T u + L_t u^T z + z^T L_t u + z^T z} \quad (8)$$

Knowing that:

$$u = (\cos\eta\,,\ \cos\gamma\,,\ \cos\xi) u = (\cos\eta\,,\ \cos\gamma\,,\ \cos\xi) \quad (9)$$

Then: $u^T u = \cos^2\eta + \cos^2\gamma + \cos^2\xi = 1 u^T u = \cos^2\eta + \cos^2\gamma + \cos^2\xi = 1$ and

$$L_t u^T z = z^T L_t u L_t u^T z = z^T L_t u \quad (10)$$

Substituting (10) into (8):

$$\|l'\| = \sqrt{{L_t}^2 + 2L_t z^T u + z^T z} \|l'\| = \sqrt{{L_t}^2 + 2L_t z^T u + z^T z} \quad (11)$$

Substituting (7) and (11) into (5):

$$\varepsilon = \frac{\sqrt{{L_t}^2 + 2L_t z^T u + z^T z} - L_t}{L_t} \varepsilon = \frac{\sqrt{{L_t}^2 + 2L_t z^T u + z^T z} - L_t}{L_t} \Rightarrow\Rightarrow \varepsilon = \sqrt{1 + {L_t}^{-1} z^T (2u + {L_t}^{-1} z)} - 1$$

$$\varepsilon = \sqrt{1 + {L_t}^{-1} z^T (2u + {L_t}^{-1} z)} - 1 \quad (12)$$

Let:

$$\delta = L_t^{-1} z^T (2u + L_t^{-1} z) \delta = L_t^{-1} z^T (2u + L_t^{-1} z) \quad (13)$$

Thus, the longitudinal strain of a cable element will be:

$$\varepsilon = \sqrt{1+\delta} - 1 \varepsilon = \sqrt{1+\delta} - 1 \quad (14)$$

TOTAL POTENTIAL ENERGY

The strain energy for a cable element with constant strain is given by:

$$\pi = \int_V \left[\int_0^{\varepsilon} \sigma(\varepsilon)\, d\varepsilon \right] dV \pi = \int_V \left[\int_0^{\varepsilon} \sigma(\varepsilon)\, d\varepsilon \right] dV \quad (15)$$

where $\sigma(\varepsilon)\sigma(\varepsilon)$ is the stress in the cable element, $\varepsilon\varepsilon$ the longitudinal strain, and e V the volume of the cable element.

For a cable element with constant cross-section (αc) and undeformed length with thermal effect (Lt), the strain energy will be:

$$\pi = \alpha_c L_t \int_0^{\varepsilon} \sigma(\varepsilon) d\varepsilon \pi = \alpha_c L_t \int_0^{\varepsilon} \sigma(\varepsilon) d\varepsilon \quad (16)$$

The Total Potential Energy for a set of n cable elements is given by:

$$\Pi(x) = \sum_{i=1}^{n} \pi - f^T x + \Pi_0 \Pi(x) = \sum_{i=1}^{n} \pi - f^T x + \Pi_0 \quad (17)$$

where $\pi\pi$ is the strain energy for each cable element, *f* is the vector containing the external nodal forces, *x* is the vector with the free nodal displacements of the system, and $\Pi_0\Pi_0$ is the initial potential energy of the system.

GRADIENT OF THE TOTAL POTENTIAL ENERGY

The gradient of the Total Potential Energy function for an arrangement of *n* tensioned cables is given by the derivative with respect to the free displacements (x_i) of the system, as follows:

$$\nabla\Pi(x) = \frac{\partial\Pi(x)}{\partial x_i} = \sum_{i=1}^{n}\nabla\pi - f\nabla\Pi(x) = \frac{\partial\Pi(x)}{\partial x_i} = \sum_{i=1}^{n}\nabla\pi - f \quad (18)$$

In this case, it is necessary to calculate the strain energy gradient ($\nabla\pi\nabla\pi$) for a cable element:

$$\nabla\pi = \alpha_c L_t \nabla\int_0^{\varepsilon}\sigma(\varepsilon)d\varepsilon\nabla\pi = \alpha_c L_t \nabla\int_0^{\varepsilon}\sigma(\varepsilon)d\varepsilon \quad (19)$$

$$\nabla\pi = \alpha_c L_t \sigma(\varepsilon)\nabla\varepsilon\nabla\pi = \alpha_c L_t \sigma(\varepsilon)\nabla\varepsilon \quad (20)$$

The strain gradient of equation (20) is given as a function of the six degrees of freedom (three translations per node) of the cable element.

As demonstrated in equation (14):

$$\varepsilon = \sqrt{1+\delta} - 1\varepsilon = \sqrt{1+\delta} - 1 \quad (21)$$

Consequently: $\nabla\varepsilon = \frac{\partial\varepsilon}{\partial x_k} = \frac{1}{2}(1+\delta)^{-1/2}\frac{\partial\delta}{\partial x_k}$

$$\nabla\varepsilon = \frac{\partial\varepsilon}{\partial x_k} = \frac{1}{2}(1+\delta)^{-1/2}\frac{\partial\delta}{\partial x_k} \quad (22)$$

With equations (3), (9), and (13), one has:

$$\delta = L_t^{-1}z^T\left(2u + L_t^{-1}z\right) = 2L_t^{-1}z^Tu + L_t^{-2}z^Tz$$

$u = (\cos\eta,\ \cos\gamma,\ \cos\xi)u = (\cos\eta,\ \cos\gamma,\ \cos\xi)$ and

$$z = q - p + c - \gamma_t lz = q - p + c - \gamma_t l$$

$$z = \{[x_4 - x_1 + (\mu - \mu_t)\cos\eta],\ [x_5 - x_2 + (\mu - \mu_t)\cos\gamma],\ [x_6 - x_3 + (\mu - \mu_t)\cos\xi]\}$$

$z = \{[x_4 - x_1 + (\mu - \mu_t)\cos\eta],\ [x_5 - x_2 + (\mu - \mu_t)\cos\gamma],\ [x_6 - x_3 + (\mu - \mu_t)\cos\xi]\}$

Let $k = 1$:

$$\frac{\partial\delta}{\partial x_1} = 2L_t^{-1}\frac{\partial}{\partial x_1}(z^Tu) + L_t^{-2}\frac{\partial}{\partial x_1}(z^Tz)\frac{\partial\delta}{\partial x_1} = 2L_t^{-1}\frac{\partial}{\partial x_1}(z^Tu) + L_t^{-2}\frac{\partial}{\partial x_1}(z^Tz)$$

(23)

but:

$$z^Tu = [x_4 - x_1 + (\mu - \mu_t)\cos\eta]\cos\eta +$$

$$[x_5 - x_2 + (\mu - \mu_t)\cos\gamma]\cos\gamma +$$

$$[x_6 - x_3 + (\mu - \mu_t)\cos\xi]\cos\xi \qquad [x_6 - x_3 + (\mu - \mu_t)\cos\xi]\cos\xi$$ and

$$z^Tz = [x_4 - x_1 + (\mu - \mu_t)\cos\eta]^2 + z^Tz = [x_4 - x_1 + (\mu - \mu_t)\cos\eta]^2 +$$

$$[x_5 - x_2 + (\mu - \mu_t)\cos\gamma]^2 +$$

$$[x_6 - x_3 + (\mu - \mu_t)\cos\xi]^2$$

Therefore:

$$\frac{\partial}{\partial x_1}(z^T u) = -\cos\eta \frac{\partial}{\partial x_1}(z^T u) = -\cos\eta \quad (24) \quad \text{e}$$

$$\frac{\partial}{\partial x_1}(z^T z) = -2[x_4 - x_1 + (\mu - \mu_t)\cos\eta] \frac{\partial}{\partial x_1}(z^T z) = -2[x_4 - x_1 + (\mu - \mu_t)\cos\eta] \quad (25)$$

Substituting equations (24) and (25) into equation (23), one obtains:

$$\frac{\partial \delta}{\partial x_1} = -2L_t^{-1}\{\cos\eta + L_t^{-1}[x_4 - x_1 + (\mu - \mu_t)\cos\eta]\}$$

$$\frac{\partial \delta}{\partial x_1} = -2L_t^{-1}\{\cos\eta + L_t^{-1}[x_4 - x_1 + (\mu - \mu_t)\cos\eta]\} \quad (26)$$

$$\frac{\partial \varepsilon}{\partial x_1} = -L_t^{-1}(1+\delta)^{-1/2}\{\cos\eta + L_t^{-1}[x_4 - x_1 + (\mu - \mu_t)\cos\eta]\}$$

$$\frac{\partial \varepsilon}{\partial x_1} = -L_t^{-1}(1+\delta)^{-1/2}\{\cos\eta + L_t^{-1}[x_4 - x_1 + (\mu - \mu_t)\cos\eta]\} \quad (27)$$

Proceeding analogously for $k = 2, 3, 4, 5$ e 6, one obtains:

$$\frac{\partial \varepsilon}{\partial x_2} = -L_t^{-1}(1+\delta)^{-1/2}\{\cos\gamma + L_t^{-1}[x_5 - x_2 + (\mu - \mu_t)\cos\gamma]\}$$

$$\frac{\partial \varepsilon}{\partial x_2} = -L_t^{-1}(1+\delta)^{-1/2}\{\cos\gamma + L_t^{-1}[x_5 - x_2 + (\mu - \mu_t)\cos\gamma]\} \quad (28)$$

$$\frac{\partial \varepsilon}{\partial x_3} = -L_t{}^{-1}(1+\delta)^{-1/2}\{cos\,\xi + L_t{}^{-1}[x_6 - x_3 + (\mu - \mu_t)\,cos\,\xi]\}$$

$$\frac{\partial \varepsilon}{\partial x_3} = -L_t{}^{-1}(1+\delta)^{-1/2}\{cos\,\xi + L_t{}^{-1}[x_6 - x_3 + (\mu - \mu_t)\,cos\,\xi]\} \quad (29)$$

$$\frac{\partial \varepsilon}{\partial x_4} = -\frac{\partial \varepsilon}{\partial x_1 \partial x_4} = -\frac{\partial \varepsilon}{\partial x_1} \quad (30)$$

$$\frac{\partial \varepsilon}{\partial x_5} = -\frac{\partial \varepsilon}{\partial x_2 \partial x_5} = -\frac{\partial \varepsilon}{\partial x_2} \quad (31)$$

$$\frac{\partial \varepsilon}{\partial x_6} = -\frac{\partial \varepsilon}{\partial x_3 \partial x_6} = -\frac{\partial \varepsilon}{\partial x_3} \quad (32)$$

The strain energy gradient ($\nabla\pi\nabla\pi$) for the cable element, considering linear elastic material ($\sigma = E\varepsilon\sigma = E\varepsilon$), will be:

$$\frac{\partial \pi}{\partial x_1} = -\alpha_c E\varepsilon(1+\delta)^{-1/2}\{cos\,\eta + L_t{}^{-1}[x_4 - x_1 + (\mu - \mu_t)\,cos\,\eta]\}$$

$$\frac{\partial \pi}{\partial x_1} = -\alpha_c E\varepsilon(1+\delta)^{-1/2}\{cos\,\eta + L_t{}^{-1}[x_4 - x_1 + (\mu - \mu_t)\,cos\,\eta]\} \quad (33)$$

$$\frac{\partial \pi}{\partial x_2} = -\alpha_c E\varepsilon(1+\delta)^{-1/2}\{cos\,\gamma + L_t{}^{-1}[x_5 - x_2 + (\mu - \mu_t)\,cos\,\gamma]\}$$

$$\frac{\partial \pi}{\partial x_2} = -\alpha_c E\varepsilon(1+\delta)^{-1/2}\{cos\,\gamma + L_t{}^{-1}[x_5 - x_2 + (\mu - \mu_t)\,cos\,\gamma]\} \quad (34)$$

$$\frac{\partial \pi}{\partial x_3} = -\alpha_c E\varepsilon(1+\delta)^{-1/2}\{cos\,\xi + L_t{}^{-1}[x_6 - x_3 + (\mu - \mu_t)\,cos\,\xi]\}$$

$$\frac{\partial \pi}{\partial x_3} = -\alpha_c E\varepsilon(1+\delta)^{-1/2}\{cos\,\xi + L_t{}^{-1}[x_6 - x_3 + (\mu - \mu_t)\,cos\,\xi]\} \quad (35)$$

$$\frac{\partial \pi}{\partial x_4} = -\frac{\partial \pi}{\partial x_1}\frac{\partial \pi}{\partial x_4} = -\frac{\partial \pi}{\partial x_1} \quad (36)$$

$$\frac{\partial \pi}{\partial x_5} = -\frac{\partial \pi}{\partial x_2}\frac{\partial \pi}{\partial x_5} = -\frac{\partial \pi}{\partial x_2} \quad (37)$$

$$\frac{\partial \pi}{\partial x_6} = -\frac{\partial \pi}{\partial x_3}\frac{\partial \pi}{\partial x_6} = -\frac{\partial \pi}{\partial x_3} \quad (38)$$

LINEAR MODEL FOR TENSIONED CABLE

LONGITUDINAL STRAIN

The longitudinal strain of the cable element for the linear model can be represented by:

$$\varepsilon = \frac{\Delta L}{L_t}\varepsilon = \frac{\Delta L}{L_t} \quad (39)$$

where $\Delta L \Delta L$is the variation in cable length and $L_t L_t$ s the undeformed length of the cable with thermal effect.

The relationships shown in equations (3) and (4) can be represented vectorially for the linear tensioned cable model as follows (Figure 3).

Figure 3

Vector representation of the linear cable element model (Menin [3])

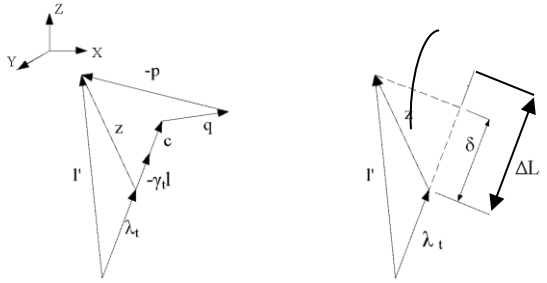

Since the displacements and strains are infinitesimal, the variation in cable length ($\Delta L \Delta L$) can be approximated by the projection (δ) of vector (z) in the direction of the cable in the undeformed configuration ($\lambda_t \lambda_t$). Thus, we have:

$$\delta = z^T u \delta = z^T u \quad \Rightarrow\Rightarrow \quad \varepsilon = \frac{\Delta L}{L_t} = \frac{\delta}{L_t} \varepsilon = \frac{\Delta L}{L_t} = \frac{\delta}{L_t} \tag{40}$$

TOTAL POTENTIAL ENERGY

For a cable element with constant cross-section (α_c) and length (L_t),the representation of the potential energy is of the same form as equation (16), previously obtained from the nonlinear model.

$$\pi = \alpha_c L_t \int_0^{\varepsilon} \sigma(\varepsilon) d\varepsilon \pi = \alpha_c L_t \int_0^{\varepsilon} \sigma(\varepsilon) d\varepsilon \tag{41}$$

GRADIENT OF THE TOTAL POTENTIAL ENERGY

Thus, the gradient of the Total Potential Energy for a cable element is given according to equation (20). Therefore, the strain gradient ($\nabla \varepsilon \nabla \varepsilon$) can be expressed as:

$$\nabla \varepsilon = \frac{\partial \varepsilon}{\partial x_k} = \frac{1}{L_t} \frac{\partial \delta}{\partial x_k} \nabla \varepsilon = \frac{\partial \varepsilon}{\partial x_k} = \frac{1}{L_t} \frac{\partial \delta}{\partial x_k} \tag{42}$$

However, as demonstrated in equation (24) for $k = 1$, and substituting (43) into (42), one obtains:

$$\frac{\partial \delta}{\partial x_1} = \frac{\partial}{\partial x_1}(z^T u) = -\cos \eta \frac{\partial \delta}{\partial x_1} = \frac{\partial}{\partial x_1}(z^T u) = -\cos \eta \tag{43} \quad \Rightarrow\Rightarrow$$

$$\frac{\partial \varepsilon}{\partial x_1} = -\frac{1}{L_t} \cos \eta \frac{\partial \varepsilon}{\partial x_1} = -\frac{1}{L_t} \cos \eta \tag{44}$$

Analogously, for k = 2, 3, 4, 5 and 6, we have:

$$\frac{\partial \varepsilon}{\partial x_2} = -\frac{1}{L_t}\cos\gamma \frac{\partial \varepsilon}{\partial x_2} = -\frac{1}{L_t}\cos\gamma \quad (45)$$

$$\frac{\partial \varepsilon}{\partial x_3} = -\frac{1}{L_t}\cos\xi \frac{\partial \varepsilon}{\partial x_3} = -\frac{1}{L_t}\cos\xi \quad (46)$$

$$\frac{\partial \varepsilon}{\partial x_4} = -\frac{\partial \varepsilon\ \partial \varepsilon}{\partial x_1 \partial x_4} = -\frac{\partial \varepsilon}{\partial x_1} \quad (47)$$

$$\frac{\partial \varepsilon}{\partial x_5} = -\frac{\partial \varepsilon\ \partial \varepsilon}{\partial x_2 \partial x_5} = -\frac{\partial \varepsilon}{\partial x_2} \quad (48)$$

$$\frac{\partial \varepsilon}{\partial x_6} = -\frac{\partial \varepsilon\ \partial \varepsilon}{\partial x_3 \partial x_6} = -\frac{\partial \varepsilon}{\partial x_3} \quad (49)$$

The strain energy gradient ($\nabla\pi\nabla\pi$) for the cable element will be:

$$\frac{\partial \pi}{\partial x_1} = -\alpha_c E\varepsilon\cos\eta \frac{\partial \pi}{\partial x_1} = -\alpha_c E\varepsilon\cos\eta \quad (50)$$

$$\frac{\partial \pi}{\partial x_2} = -\alpha_c E\varepsilon\cos\gamma \frac{\partial \pi}{\partial x_2} = -\alpha_c E\varepsilon\cos\gamma \quad (51)$$

$$\frac{\partial \pi}{\partial x_3} = -\alpha_c E\varepsilon\cos\xi \frac{\partial \pi}{\partial x_3} = -\alpha_c E\varepsilon\cos\xi \quad (52)$$

$$\frac{\partial \pi}{\partial x_4} = -\frac{\partial \pi\ \partial \pi}{\partial x_1 \partial x_4} = -\frac{\partial \pi}{\partial x_1} \quad (53)$$

$$\frac{\partial \pi}{\partial x_5} = -\frac{\partial \pi}{\partial x_2}\frac{\partial \pi}{\partial x_5} = -\frac{\partial \pi}{\partial x_2} \quad (54)$$

$$\frac{\partial \pi}{\partial x_6} = -\frac{\partial \pi}{\partial x_3}\frac{\partial \pi}{\partial x_6} = -\frac{\partial \pi}{\partial x_3} \quad (55)$$

STATIC WIND ANALYSIS ACCORDING TO NBR6123

The forces resulting from the incidence of wind on a structure, commonly known as aerodynamic forces, produce a horizontal component in the wind direction called drag force $-Fa$, calculated according to the equation: $Fa = Ca\ q\ AFa = Ca\ q\ A$, where Ca is the drag coefficient (aerodynamic parameter), q is the dynamic wind pressure (meteorological parameter), and A is the reference surface area (geometric parameter).

According to standard NBR6123 [1], the drag coefficient (Ca) in square-section lattice towers varies according to the exposed area index $\varphi\varphi$. This index is defined as the ratio between the effective frontal area of one of the truss faces and the total area corresponding to the surface bounded by the truss outline. It is important to emphasize that the drag coefficient (Ca) s not constant along the tower, since its value is calculated individually for each of the modules as a function of the exposed area index ($\varphi\varphi$) of the respective module.

The meteorological parameter (q) represents the variation of the dynamic wind pressure in relation to the mean velocity profile. The drag force (Fa) can be determined by considering the continuous velocity profile or, with good approximation, from a stepped profile, according to Blessmann.

The drag force (Fa) is calculated for a differential (df) of the continuous profile and integrated within the desired limit. Initially, a building with solid faces is assumed, later corrected as a function of the exposed area index $-\varphi\varphi$. According to the continuous profile in Figure 4, the drag force for a strip of width $l_1(z)$ and height dz can be expressed as:

$$dfa = Caq(z)l_1(z)dzdfa = Caq(z)l_1(z)dz \quad (56)$$

Figure 4

Drag force from the continuous profile (Blessmann [2])

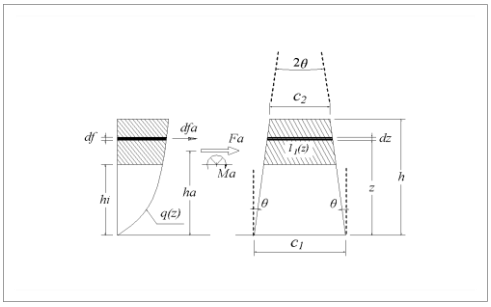

The partial drag force between the top of the building (*h*) and the lower level (*hi*), will be:

$$Fa = \int_{hi}^{h} dfaFa = \int_{hi}^{h} dfa \quad \text{or} \quad Fa = Ca \int_{hi}^{h} q(z)\ l_1(z)\ dz$$

$$Fa = Ca \int_{hi}^{h} q(z)\ l_1(z)\ dz \quad (57)$$

resulting in:

$$Fa = K_2 \rightleftharpoons Ca \rightleftharpoons \left[\frac{c_1}{2p+1}\left(h^{2p+1} - hi^{2p+1}\right) - \frac{2 \rightleftharpoons tg\theta}{2p+2}\left(h^{2p+2} - hi^{2p+2}\right)\right]\varphi$$

$$Fa = K_2 \rightleftharpoons Ca \rightleftharpoons \left[\frac{c_1}{2p+1}\left(h^{2p+1} - hi^{2p+1}\right) - \frac{2 \rightleftharpoons tg\theta}{2p+2}\left(h^{2p+2} - hi^{2p+2}\right)\right]\varphi \quad (58)$$

The distance (ha) between the point of application of the resultant force and the base is given by:

$$Fa\ ha = \int_{hi}^{h} zdfa\ Fa\ ha = \int_{hi}^{h} zdfa \quad (59)$$

resulting in:

$$ha = \frac{\frac{c_1}{2p+2}(h^{2p+2} - hi^{2p+2}) - \frac{2\ tg\theta}{2p+3}(h^{2p+3} - hi^{2p+3})}{\frac{c_1}{2p+1}(h^{2p+1} - hi^{2p+1}) - \frac{2\ tg\theta}{2p+2}(h^{2p+2} - hi^{2p+2})} ha = \frac{\frac{c_1}{2p+2}(h^{2p+2} - hi^{2p+2}) - \frac{2\ tg\theta}{2p+3}(h^{2p+3} - hi^{2p+3})}{\frac{c_1}{2p+1}(h^{2p+1} - hi^{2p+1}) - \frac{2\ tg\theta}{2p+2}(h^{2p+2} - hi^{2p+2})}$$

(60)

For the case of guyed steel towers with square cross-section subjected to a wind load incident at an angle (α) equal to 0º relative to the perpendicular to the windward face, the horizontal and vertical decompositions of the drag force (Fa) are presented in NBR6123 [1] and schematized according to Figure 5.

Figure 5

Vertical and horizontal decompositions for the drag forces (Fa)

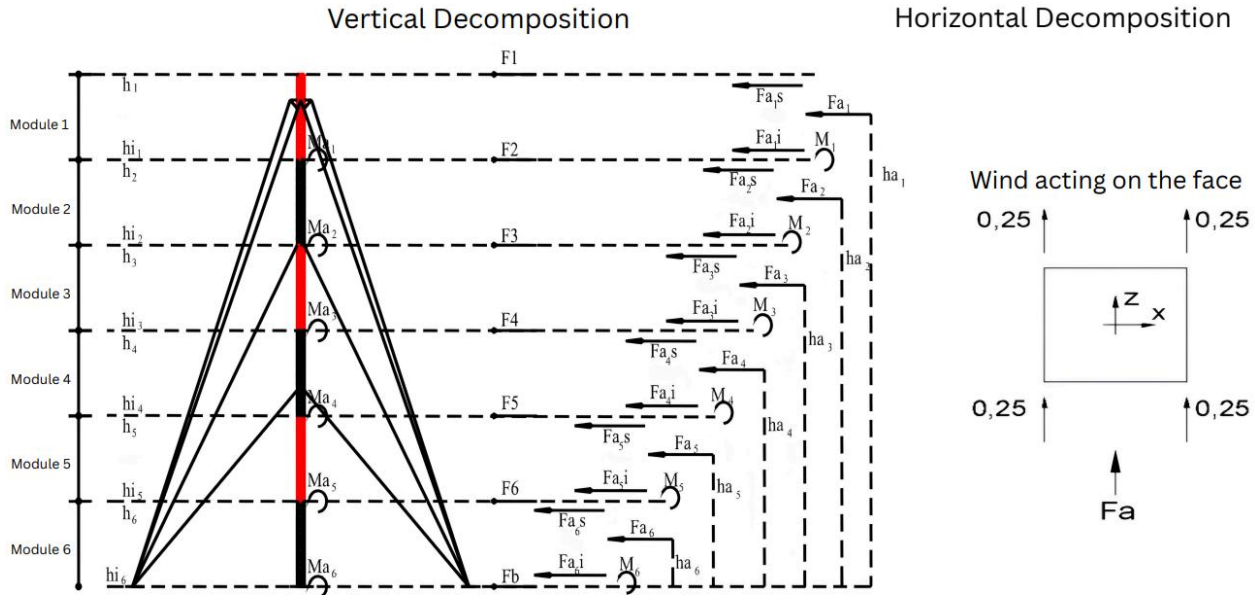

APPLICATIONS AND RESULTS

This section presents the results of the static analysis performed for guyed towers of 10 and 30 meters in height. The results were obtained through the static analysis program (AETEQ), developed by Menin. The AETEQ computational program uses the linear model for tensioned cable. The results were evaluated in terms of maximum top displacement, support reactions, and cable anchorage reactions.

In the static analysis of the guyed towers, the wind loading simulation was determined from the parameters defined in NBR6123, among them: basic wind speed equal to 45 m/s; topographic factor S_1 equal to 1.0; and the statistical factor S_3, for the case of telecommunication towers, considered equal to 1.1. Temperature variations (ΔT) in the cable and bar elements of the guyed towers were not considered in this analysis. In the AETEQ program, despite the requirements of standard NBR6123 for considering static wind action with incidence angles (α) equal to 0º and 45º from the windward face of the tower, it should be noted that in this work only the incidence angle equal to 0º was adopted (loading perpendicular to one of the faces).

The geometric dimensions of the 10- and 30-meter guyed towers and their respective silhouettes are presented in Figure 9.

Figure 9

Guyed towers of 10 and 30 meters (not to scale)

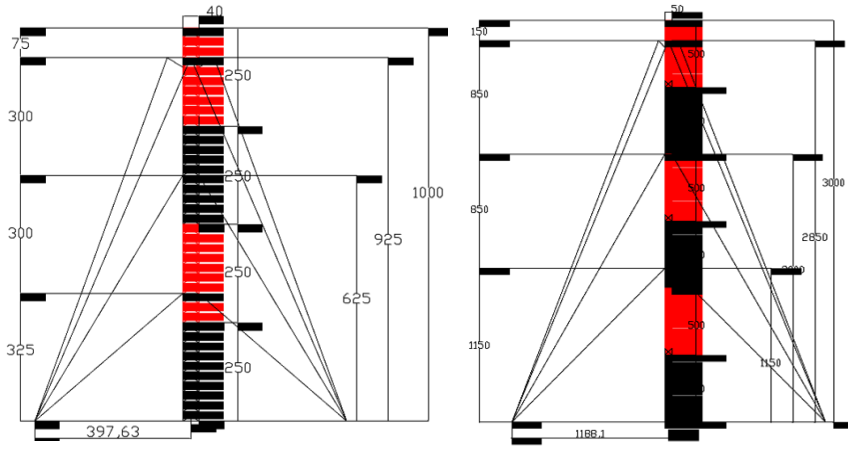

Table 2 initially presents a summary of the displacements in the direction of the wind loading, taking as reference the four nodes located at the top of the guyed towers. For the linear static analysis, the loads acting on these structures were: self-weight (PP), cable tensioning (DEF), and wind loading (CV), considered as nominal loads. In the same table, a comparison is also presented between the nodal displacements obtained through the AETEQ program and those from the SAP2000 program.

Table 2

Comparison between nodal displacements at the top of the guyed towers

Node	Nodal displacements at the top (cm)			
	10m		30m	
	AETEQ	SAP	AETEQ	SAP
1	0,4356	0,4406	2,6830	2,6848
2	0,4399	0,4448	2,6889	2,6905
3	0,4403	0,4449	2,6897	2,6906
4	0,4353	0,4400	2,6822	2,6834

From Table 2, it is observed that the displacement values of the top nodes did not present significant differences between the AETEQ and SAP2000 programs used for this analysis. The variation in results between the two programs did not exceed 1%, proving satisfactory.

Due to the large number of bar elements in the guyed towers, Table 3 presents only the maximum axial forces for the leg members (M) located at the base of these structures.

Table 3

Axial forces in the base leg members of the guyed towers

Guyed Tower	Base Legs	AETEQ	SAP2000	Difference
		Axial force (kN)	Axial force (kN)	
10m	481	-6,09751	-6,07767	0,33%
	482	-6,44483	-6,39315	0,81%
	483	-13,23699	-13,26850	0,24%
	484	-12,92826	-12,92379	0,03%
30m	725	-4,37667	-4,35033	0,61%
	726	-6,01792	-5,99745	0,34%
	727	-35,28692	-35,33454	0,13%
	728	-33,64566	-33,64946	0,01%

The results referring to the support reactions at the base of the 10- and 30-meter guyed towers, also including the cable anchorage points, are presented in Table 4. The support reaction results were obtained from the AETEQ static analysis program and subsequently compared with those from SAP2000. In Table 4, the first four nodes always correspond to the lower-end nodes of the leg members, and the remaining ones correspond to the cable anchorage points. The support reactions referring to the orthogonal x and z axes define the horizontal plane, where the z-axis comprises the direction of the wind loading and y is the vertical axis of the structure.

Table 4

Comparison between support reactions from the AETEQ and SAP2000 programs

Node	30m Guyed Tower								
	AETEQ (kN)			SAP2000 (kN)			Reactions Difference (kN and %)		
	RX	RY	RZ	RX	RY	RZ	RX	RY	RZ
241	0,0000	4,3934	0,0000	0,0056	4,3595	0,0000	-0,0056	0,0338	0,0000
							0,00%	0,78%	0,00%
242	0,0000	4,3738	-1,6769	0,0000	4,3212	-1,6799	0,0000	0,0526	0,0029
							0,00%	1,22%	0,18%
243	0,0000	35,3137	0,0000	0,0026	35,3487	0,0000	-0,0026	-0,0349	0,0000
							0,00%	0,10%	0,00%
244	0,0000	35,3334	-1,6769	0,0000	35,3459	-1,6797	0,0000	-0,0126	0,0027
							0,00%	0,04%	0,16%
249	-14,9159	-25,8013	-14,9257	-14,9120	-25,7968	-14,9218	-0,0039	-0,0045	-0,0039
							0,03%	0,02%	0,03%
250	14,9159	-25,8013	-14,9257	14,9090	-25,7972	-14,9189	0,0069	-0,0041	-0,0069
							0,05%	0,02%	0,05%
251	5,3250	-10,4245	5,3152	5,3100	-10,3918	5,3002	0,0150	-0,0327	0,0150
							0,28%	0,31%	0,28%
252	-5,3348	-10,4245	5,3250	-5,3153	-10,3929	5,3056	-0,0195	-0,0316	0,0194
							0,37%	0,30%	0,37%

Node	10m Guyed Tower					
	AETEQ (kN)			SAP2000 (kN)		
	RX	RY	RZ	RX	RY	RZ
161	0,0000	6,0997	0,0000	-0,0008	6,0788	0,0000
162	0,0000	6,1193	-0,5099	0,0000	6,0748	-0,5119
163	0,0000	13,2390	0,0000	0,0026	13,2685	0,0000
164	0,0000	13,2194	-0,5001	0,0000	13,2404	-0,5042
169	-6,4037	-11,0129	-6,4135	-6,4124	-11,0233	-6,4200
170	6,4037	-11,0129	-6,4135	6,4135	-11,0258	-6,4207
171	4,2463	-7,4334	4,2365	4,2276	-7,4142	4,2202
172	-4,2463	-7,4334	4,2365	-4,2308	-7,4155	4,2233

It is verified that, in the comparison of the values generated by the AETEQ program and the SAP2000 program, the difference between support reactions remained, in most cases, less than 1%. Thus, it can be concluded that there is a good correlation between the results obtained by the AETEQ and SAP2000 programs.

CONCLUSIONS

In the static analysis of the guyed towers, it was possible to observe that the results obtained from the AETEQ program, using the linear formulation for spatial cable elements, were very close to those

obtained through the SAP2000 program, presenting nonsignificant response variations on the order of 1%, referring to top displacements, maximum axial forces in the base leg members, and support reactions.

REFERENCES

Abubakar, M. et al. Comparative study of finite element modeling techniques for lattice telecommunication towers. *Structures*, v. 62, p. 104–118, 2024.

Altay, O. et al. Numerical investigation of the collapse mechanisms of self-supporting telecommunication towers under extreme wind loading. *Structures*, v. 60, art. 105842, 2024.

Associação Brasileira de Normas Técnicas (ABNT). *NBR 6123: forças devidas ao vento em edificações* [NBR 6123: wind loads on buildings]. Rio de Janeiro: ABNT, 1988. Confirmada em 2013.

Bathe, K. J. *Finite element procedures*. New Jersey: Prentice Hall, 1996.

Blessmann, J. *Introdução ao estudo das ações dinâmicas do vento* [Introduction to the study of dynamic wind actions]. Porto Alegre: Editora da UFRGS, 1998.

Blessmann, J. *Forças devidas ao vento em edificações altas* [Wind loads on tall buildings]. Caderno de Engenharia CE-27. Porto Alegre: CPGEC/UFRGS, 1988.

Chen, X. et al. Stochastic wind field simulation and dynamic response of guyed masts using advanced Monte Carlo techniques. *Journal of Wind Engineering and Industrial Aerodynamics*, v. 234, art. 105341, 2023.

Cook, R. D.; Malkus, D. S.; Plesha, M. E.; Witt, R. J. *Concepts and applications of finite element analysis*. 4. ed. New York: John Wiley & Sons, 2002.

Fu, X.; Li, H. et al. Wind-induced vibration analysis and structural reliability assessment of guyed transmission towers. *Engineering Structures*, v. 287, art. 116098, 2023.

Gere, J. M.; Weaver Jr., W. *Análise de estruturas reticuladas* [Analysis of truss structures]. Rio de Janeiro: LTC, 2003.

Logan, D. L. *A first course in the finite element method*. 6. ed. Stamford: Cengage Learning, 2017.

Menin, R. C. G. *Análise estática e dinâmica de torres estaiadas* [Static and dynamic analysis of guyed towers]. Dissertação (Mestrado em Estruturas) – Universidade de Brasília, Brasília, 2002.

Moraes, C. S.; Silva, A. R.; Oliveira, M. T. Modelagem computacional aplicada à análise não linear de torres metálicas estaiadas submetidas ao vento [Computational modeling applied to nonlinear analysis of guyed steel towers under wind loading]. *Revista IBRACON de Estruturas e Materiais*, v. 15, n. 4, p. 1–18, 2022.

Pulino, A. R. F. *Contribuição ao estudo das coberturas pênseis* [Contribution to the study of suspended structures]. Tese (Doutorado em Engenharia Mecânica) – Universidade Estadual de Campinas, Campinas, 1991.

Pulino, A. R. F. Notas de aula não publicadas [Unpublished lecture notes]. Universidade de Brasília, Brasília, 1998.

SAP2000. *Structural analysis program: advanced analysis reference manual*. Version 10.0.1. Berkeley: Computers and Structures Inc., 2005.

Silva, V. P.; Pimenta, P. M. *Análise não linear de estruturas* [Nonlinear structural analysis]. São Paulo: EDUSP, 2008.

Soriano, H. L. *Método dos elementos finitos em análise de estruturas* [Finite element method in structural analysis]. São Paulo: EDUSP, 2003.

Thomas, G. B.; Weir, M. D.; Hass, J. *Thomas' calculus*. 15. ed. Boston: Pearson, 2021.

Timoshenko, S. P.; Gere, J. M. *Theory of elastic stability*. 2. ed. New York: McGraw-Hill, 1961.

Zhang, Y. et al. Structural optimization and aerodynamic performance of steel lattice towers subjected to wind loads. *Journal of Constructional Steel Research*, v. 196, art. 107421, 2022.